Neoplasia • Vol. 7, No. 1, January 2005, pp. 37–47

www.neoplasia.com

Association between Pterostilbene and Quercetin Inhibits Metastatic Activity of B16 Melanoma[1]

Paula Ferrer, Miguel Asensi*, Ramón Segarra*, Angel Ortega*, María Benlloch*, Elena Obrador*, María T. Varea†, Gregorio Asensio†, Leonardo Jordá‡ and José M. Estrela**

Departments of *Physiology and †Organic Chemistry, University of Valencia, Valencia, Spain; ‡Valefarma SA, Valencia, Spain

Abstract

Inhibition of cancer growth by resveratrol (*trans*-3,5,4′-trihydroxystilbene; RESV), a phytoalexin present in many plant species, is limited by its low bioavailability. Pterostilbene (3,5-dimethoxy-4′-hydroxystilbene; PTER) and quercetin (3,3′,4′,5,6-pentahydroxyflavone; QUER), two structurally related and naturally occurring small polyphenols, show longer half-life *in vivo*. *In vitro* growth of highly malignant B16 melanoma F10 cells (B16M-F10) is inhibited (56%) by short-time exposure (60 min/day) to PTER (40 μM) and QUER (20 μM) (approximate mean values of plasma concentrations measured within the first hour after intravenous administration of 20 mg/kg of each polyphenol). Intravenous administration of PTER and QUER (20 mg/kg per day) to mice inhibits (73%) metastatic growth of B16M-F10 cells in the liver, a common site for metastasis development. The antimetastatic mechanism involves: 1) a PTER-induced inhibition of vascular adhesion molecule 1 expression in the hepatic sinusoidal endothelium, which consequently decreases B16M-F10 cell adhesion to the endothelium through very late activation antigen 4; and 2) a QUER- and PTER-induced inhibition of Bcl-2 expression in metastatic cells, which sensitizes them to vascular endothelium-induced cytotoxicity. Our findings demonstrate that the association of PTER and QUER inhibits metastatic melanoma growth and extends host survival.

Neoplasia (2005) **7,** 37–47

Keywords: Polyphenols, pterostilbene, quercetin, melanoma, metastases.

Introduction

Different phenolic compounds, including resveratrol (RESV), show potent antioxidant effects and may have therapeutic applications in oxidative stress–related diseases such as cancer [1–3]. The cancer chemopreventive activity of RESV was first reported by Jang et al. [4]. The mechanisms by which RESV exerts its antitumor effects are under active investigation [3] and may include, for example: 1) inhibition of ribonucleotide reductase [5], DNA polymerase [6], protein kinase C [7], or cyclooxygenase-2 [8] activities; 2) inhibition of reactive oxygen species–mediated carcinogenesis [4] or cell proliferation [9]; and 3) apoptotic cell death activation [10–13]. However, potential inhibition of cancer growth by RESV is strongly limited due to its low bioavailability [14]. Thus, structural modifications of the RESV molecule to increase its bioavailability while preserving its biologic activity appeared necessary. The 4′-OH and stereoisometry in its *trans*-conformation are absolutely required for inhibition of cell proliferation [15]. Pterostilbene (PTER), a naturally occurring analogue of RESV but is about 60 to 100 times stronger as an antifungal agent, shows similar anticarcinogenic properties [16]. Besides, flavonoids are among the most potent antioxidants because they show one or more of the following structural elements: an *o*-diphenolic group, two to three double bonds conjugated with the 4-oxo function, and OH groups in positions 3 and 5. Quercetin (QUER) combines all these three properties, and previous research has confirmed that it also exhibits antitumor properties, likely due to immune stimulation, free radical scavenging, alteration of the mitotic cycle in tumor cells, gene expression modification, antiangiogenesis activity, apoptosis induction, or a combination of these effects [2,17]. Because potential anticancer effects induced by natural polyphenols still have not been proven effective by systemic administration, we investigated the anticancer properties of PTER and QUER at bioavailable concentrations. We found that their association strongly inhibits the metastatic growth of the highly malignant B16 melanoma.

Abbreviations: B16M-F10, B16 melanoma F10; RESV, resveratrol; t-RESV, *trans*-resveratrol; PTER, pterostilbene; t-PTER, *trans*-pterostilbene; QUER, quercetin; HSE, hepatic sinusoidal endothelium; VCAM-1, vascular adhesion molecule 1; VLA-4, very late activation antigen 4; B16M-F10/Tet-Bcl-2, Bcl-2–overexpressing B16 melanoma F10; LC-MS/MS, high-pressure liquid chromatography and mass spectrometry

Address all correspondence to: Dr. José M. Estrela, Department of Physiology, Faculty of Medicine, Av. Blasco Ibañez 17, Valencia 46010, Spain. E-mail: jose.m.estrela@uv.es

[1]This research was supported by grants from the Ministerio de Educación y Ciencia (MEC; VIN01-013 and SAF2003-01886), the Generalitat Valenciana (GVA; GRUPOS03/185), Valefarma SA, Secna SA, and Universal Armony SL (Spain). P. Ferrer and M. Benlloch held fellowships from the MEC, whereas A. L. Ortega held a fellowship from the GVA (Spain).
Received 21 May 2004; Revised 12 July 2004; Accepted 13 July 2004.

DOI 10.1593/neo.04337

Materials and Methods

Animals and In Vivo Administration of Polyphenols

Mice (C57BL/6J, male, 6–8 weeks) were from Charles River Spain (Barcelona, Spain). Procedures involving animals and their care were conducted in conformity with institutional guidelines that are in compliance with the national and international laws and policies (European Community Council Directive 86/609, OJ L 358. 1, December 12, 1987) and the National Institutes of Health (USA) Guide for the Care and Use of Laboratory Animals (NIH Publ. No. 85-23, 1985). All animals were fed *ad libitum* on stock laboratory diets (Letica, Barcelona, Spain) and kept on a 12-hour light/12-hour dark cycle with the room temperature maintained at 22°C. Experiments were started at 10:00 A.M. to minimize the effects of diurnal variation.

For pharmacokinetic studies and daily treatment, 20 mg of t-PTER (dissolved in 0.5 ml of ethanol) or QUER (dissolved in 0.15 ml of dimethylsulfoxide/physiological saline, 1:0.5) per kilogram was administered intravenously (through the jugular vein where, previously, a permanent catheter was surgically fixed; intravenous administration was slowly performed during 1 minute) or orally (through an intragastric tube) to mice. t-PTER was synthesized in our laboratory following standard Wittig and Heck reactions (www.orgsyn.org), whereas QUER was obtained from Sigma Chemical Co. (St. Louis, MO). ^{3}H-t-PTER (2.2 Ci/mmol), labelled in *ortho* and *para* of benzenic rings, was prepared in our laboratory following a method similar to that used for deuteriation of phenols [18]. ^{14}C-QUER (50 mCi/mmol), labelled in the 4-position of the C-ring, was obtained from the NCI Radiochemical Carcinogen Repository at Chemsyn Laboratories (Kansas City, MO). Radioactivity was measured using a Packard 2700TR Varisette analyzer. Blood was collected through the catheter into 1-ml syringes containing sodium heparin (0.05 ml of a 5% solution in 6.9% NaCl). Plasma and erythrocytes were separated as previously described [19].

Determination of PTER and QUER by Liquid Chromatography and Mass Spectrometry (LC-MS/MS)

LC-MS/MS was carried out using a Quattro Micro triple–quadrupole mass spectrometer (Micromass, Manchester, UK) equipped with a Shimadzu LC-10ADvp. pump and a SLC-10Avp. controller system with a SIL-10ADvp. autoinjector. Samples were analysed by reverse-phase high-pressure liquid chromatography using a Phenomenex (Torrance, CA) Prodigy ODS column (100×2 mm) with 3 μm particle size. In all cases, 40 μl was injected onto the column. The temperature of the column was maintained at 25°C. The following gradient system, pumped through the column at 0.2 ml/min, was used (min/%A /% B/% C) (A, methanol; B, 10% acetonitrile and 90% 10 mM ammonium formate, pH 3.75; C, 10 mM ammonium formate, pH 3.75): 0/5/5/90, 10/5/5/90, 20/5/90/5, 30/100/0/0, and 40/5/5/90. Negative ion electrospray tandem mass spectra were recorded with the electrospray capillary set at 3.5 keV and a source block temperature of 120°C. Nitrogen was used as the drying and nebulizing gas at flow rates of 300 and 30 l/hr, respectively. Argon at 1.5×10^{-3} mbar was used as the collision gas for collision-induced dissociation. An assay based on LC-MS/MS with multiple reaction monitoring was developed using the transitions *m/z* 255 to 240 for PTER and 300 to 151 for QUER, both of which represent favorable fragmentation pathways for these deprotonated molecules. Calibration curves were obtained using a standard of PTER or QUER (0.01–100 μM) and, in each case, were found to be linear with correlation coefficients > 0.99. The limits of detection and quantitation for our method were of 0.01 μM.

Culture of Tumor Cells

B16M derived from B16M-F10 subline cells were cultured [20] in Dulbecco's modified Eagle's medium (DMEM; Gibco Laboratories, Grand Island, NY), pH 7.4, supplemented with 10 % fetal calf serum (Gibco Laboratories), 10 mM HEPES, 40 mM $NaHCO_3$, 100 U/ml penicillin, and 100 μg/ml streptomycin.

Isolation and Culture of Hepatic Sinusoidal Endothelium (HSE)

Male C57BL/6J mice (10–12 weeks old) were from IFFA Credo (L'Arbreole, France) and received care according to the criteria outlined by the NIH. HSE was separated and identified as previously described [20]. Sinusoidal cells were separated in a 17.5% (wt/vol) metrizamide gradient. Cultures of HSE were established and maintained in pyrogen-free DMEM supplemented as described above for the B16M-F10 cells. Differential adhesion of endothelial cells to the collagen matrix and washing allow a complete elimination of other sinusoidal cell types (Kupffer, stellate, and lymphocytes) from the culture flasks.

B16 Melanoma–Endothelial Cell Adhesion and Cytotoxicity Assays

B16M-F10 cells were loaded with 2′,7′-bis-(2-carboxyethyl)-5,6-carboxyfluorescein acetoxymethylester (BCECF-AM; Molecular Probes, Eugene, OR) (10^6 cells were incubated in 1 ml of HEPES-buffered DMEM, containing 50 μg of BCECF-AM and 5 μl of DMSO, during 20 minutes at 37°C). After washing, BCECF-AM–containing cells were resuspended in HEPES-buffered DMEM without phenol red at a concentration of 2.5×10^6 cells/ml, and added (0.2 ml/well) to endothelial cells (plated 24 hours before) and also to plastic- or collagen-precoated control wells. The plates were then incubated at 37°C and, 20 minutes later, the wells were washed three times with fresh medium and read for fluorescence using a Fluoroskan Ascent FL (Labsystems, Manchester, UK). The number of adhering tumor cells was quantified by arbitrary fluorescence units based on the percentage of the initial number of B16M-F10 cells added to the HSE culture [20]. Damage to B16M-F10 cells during their *in vitro* adhesion to the HSE was measured, as previously described [21], using tumor cells loaded with calcein-AM (Molecular Probes). The integrity of B16M-F10 cells cultured alone was assessed by trypan blue exclusion and by measuring lactate dehydrogenase activity released to the extracellular

medium [22]. Other reagents used in experiments of tumor cytotoxicity were from Sigma.

Cytokines

Recombinant murine TNF-α (2×10^7 U/mg protein) and recombinant murine interferon-γ (IFN-γ; 10^5 U/mg protein) were obtained from Sigma. Stock solutions (5×10^5 U of TNF-α/ml and 25×10^4 U of IFN-γ/ml) were diluted in sterile physiological saline solution (0.9 % NaCl), adjusted to pH 7.0, and stored at 4°C.

Assay for In Vitro Invasion of Hepatic Endothelial Cell Monolayer by B16 Melanoma Cells

Invasion of endothelial cell monolayer by B16M-F10 cells was assayed in accordance with the method by Ohigashi et al. [23] with some modifications. HSE cells were seeded on (1%) gelatin-coated tissue culture dishes with grids. When the cells reached confluency, the culture medium was replaced with fresh medium. After a 2-hour incubation, the cultures were washed with DMEM and then B16M-F10 cells were cultured on overlayered HSE cells for 5 days. The invasion capacity of B16M-F10 cells was measured by counting the number of colonies per 1 cm^2 formed under the HSE monolayer using a phase contrast microscope.

Calculation of the Interaction Index of a Combination

The method used is described by Berenbaum [24] where the interactive response for a combination of two compounds is expressed as: $dA/DA + dB/DB = 1$, where *d*A and *d*B represent values of concentrations of two agents (A and B) in combination (40 μM t-PTER and 20 μM QUER, in our case; see the legend to Figure 2). Dose–response curves of agents A and/or B (where the *y*-axis represents the percent of inhibition of cell growth *in vitro* and the *x*-axis represents the concentration of each polyphenol) will indicate at which concentrations A, B, and A + B are isoeffective. If the equation results in a value significantly less than one, synergism will be inferred; if more, then antagonism will be inferred.

Measurement of H_2O_2, Nitrite, and Nitrate

The assay of H_2O_2 production was based on the H_2O_2-dependent oxidation of homovanillic acid (3-methoxy-4-hydroxyphenylacetic acid) to a highly fluorescent dimer (2,2′-dihydroxydiphenyl-5,5′-diacetic acid), which is mediated by horseradish peroxidase [20]. For this purpose, cells were cultured in the presence of 100 μM homovanillic acid and 1 U/ml horseradish peroxidase. A linear relationship between fluorescence ($\lambda_{excitation}$ = 312 nm and $\lambda_{emission}$ = 420 nm) and amount of H_2O_2 was found in the range of 0.1 to 12 nmol per 2-ml assay.

Nitrite and nitrate determinations were performed using the methodology of Braman and Hendrix [25]. Briefly, measurement of NO_2^- levels were made by monitoring NO evolution through chemiluminescence detection from a measured sample placed into a refluxing solution of iodide/acetic acid (which will only reduce NO_2^- and not NO_3^- to NO). Total NO_x (NO_2^- plus NO_3^-) determinations were made by monitoring NO evolution from a measured sample placed into a boiling VCl_3/HCl solution (which will reduce both NO_2^- and NO_3^- to NO). The determination of NO_3^- levels was made by subtracting the value for NO_2^- from the NO_x value. Quantitation was accomplished using a standard curve made up of known amounts of NO_2^- and NO_3^-.

Flow Cytometry

Expression of intercellular adhesion molecules was analyzed by flow cytometry [26]. For this purpose, B16M-F10 cells (1×10^6) were incubated with 1 μg of antimouse very late activation antigen 4 (VLA-4) monoclonal antibody (type rat IgG2b, clone PS/2; Serotec, Oxford, UK) for 1 hour at 4°C. HSE (1×10^6 cells) was incubated with 2 μg of antimouse vascular adhesion molecule 1 (VCAM-1) monoclonal antibody (type rat IgG, kappa, clone M/K-2; R&D Systems, Minneapolis, MN). B16M-F10 and HSE cells were washed with PBS twice, then were treated with fluorescein isothiocyanate–labeled goat antirat immunoglobulin antibody (Serotec) for 1 hour at 4°C. After washing with PBS twice, the cells were analyzed on a fluorescence-activated cell sorter (FACScan; Becton Dickinson, Sunnyvale, CA). Proliferation and/or viability of B16M-F10 and HSE cells was not affected by these monoclonal antibodies (even by adding up to 100 μg/ml antibody to the culture medium) (data not shown).

RT-PCR and Detection of mRNA Expression

Total RNA was isolated using the Trizol kit from Invitrogen (San Diego, CA) and following manufacturer's instructions. cDNA was obtained using a random hexamer primer and a MultiScribe Reverse Transcriptase kit as described by the manufacturer (TaqMan RT Reagents; Applied Biosystems, Foster City, CA). A PCR master mix and AmpliTaq Gold DNA polymerase (Applied Biosystems) were then added containing the specific primers:

BAX	Forward 5′-AAGCTGAGCGAGTGTCTCCGGCG
	Reverse 5′-GCCACAAAGATGGTCACTGTCTGCC
BAK	Forward 5′-AGTGAGGGCAGAGGTGAGAGTICA
	Reverse 5′-CACAGTTGCTTCTGCTGGAGTAGTT
BAD	Forward 5′-CCAGTGATCTTCTGCTCCACATCCC
	Reverse 5′-CAACTTAGCACAGGCACCCGAGGG
BID	Forward 5′-ACAAGGCCATGCTGATAATGACAAT
	Reverse 5′-CAGATACACTCAAGCTGAACGCAG
Bcl-2	Forward 5′-CTCGTCGCTACCGTCGTGACTTCG
	Reverse 5′-CAGATGCCGGTTCAGGTACTCAGTC
Bcl-w	Forward 5′-CGAGTTTGAGACCCGTTTCCGCC
	Reverse 5′-GCACTTGTCCCACCAAAGGCTCC
Bcl-xL	Forward 5′-TGGAGTAAACTGGGGGTCGCATCG
	Reverse 5′-AGCCACCGTCATGCCCGTCAGG
GAPDH	Forward 5′-CCTGGAGAAACCTGCCAAGTATG
	Reverse 5′-GGTCCTCAGTGTAGCCCAAGATG

Real-time quantitation of each mRNA relative to glyceraldehyde-3P-dehydrogenase (GAPDH) mRNA was performed with an SYBR Green I assay and an iCycler

detection system (BioRad, Hercules, CA). Target cDNA were amplified in separate tubes using the following: 10 minutes at 95°C, then 40 cycles of amplification (denaturation at 95°C for 30 seconds, and annealing and extension at 60°C for 1 minute per cycle). The increase in fluorescence was measured in real time during the extension step. The threshold cycle (C_T) was determined, and then the relative gene expression was expressed as: fold change = $2^{-\Delta(\Delta C_T)}$, where $\Delta C_T = C_T$ target $- C_T$ GAPDH, and $\Delta(\Delta C_T) = \Delta C_T$ treated $- \Delta C_T$ control.

Bcl-2 Gene Transfer and Analysis

The Tet-off gene expression system (Clontech, Palo Alto, CA) was used, as previously reported [27], to insert the mouse *Bcl-2* gene and for transfection into B16M-F10 cells following the manufacturer's instructions. Bcl-2 protein was quantitated in the soluble cytosolic fraction by enzyme immunoassay [28] using a monoclonal antibody-based assay from Sigma (one unit of Bcl-2 was defined as the amount of Bcl-2 protein in 1000 nontransfected B16M cells).

Western Blots

Cultured cells were harvested, as indicated above, and then washed twice in ice-cold Krebs-Henseleit bicarbonate medium (pH 7.4). Whole cell extracts were made by freeze–thaw cycles in a buffer containing 150 mM NaCl, 1 mM EDTA, 10 mM Tris–HCl, 1 mM phenylmethylsulfonyl fluoride, 1 μg/ml leupeptin, 1 μg/ml aprotinin, and 1 μg/ml pepstatin, pH 7.4. Fifty micrograms of protein (as determined by the Bradford assay) were boiled with Laemmli buffer and resolved in 12.5% sodium dodecyl sulfate polyacrylamide gel electrophoresis. Proteins were transferred to a nitrocellulose membrane and subjected to Western blotting with antimouse Bcl-2 monoclonal antibody (clone YTH-10C4; Trevigen, Gaithersburg, MD). Blots were developed using horseradish peroxidase–conjugated secondary antibody and enhanced chemiluminiscence (ECL system; Amersham, Arlington Heights, IL).

Experimental Metastases

Hepatic metastases were produced by intravenous injection (portal vein) into anesthesized mice (Nembutal; 50 mg/kg ip) of 4×10^5 viable B16M-F10 cells suspended in 0.2 ml of DMEM. Mice were cervically dislocated 10 days after B16M-F10 inoculation. The livers were fixed with 10% formaldehyde in PBS (pH 7.4) for 24 hours at 22°C and then paraffin-embedded. Metastasis density (mean number of foci/100 mm^3 of liver detected in fifteen 10×10 mm^2 sections per liver) and metastasis volume (mean percent of liver volume occupied by metastasis) were determined as earlier described [22].

In vivo microscopy to follow metastatic cell dynamics within the liver was performed, as earlier described [21], using calcein-AM–labeled (Molecular Probes) B16M-F10 cells. The total number of calcein-AM–labeled cells per hepatic lobule was recorded in 10 different lobules per liver at 15-minute intervals for a 6-hour period. The microscope was an Eclipse E600FN, providing transillumination or epiillumination, equipped for video microscopy using a digital DXM 1200 camera (Nikon, Tokyo, Japan).

Isolation of B16M-F10 Cells from Liver Metastases and Determination of Cell Volume

Invasive B16M-F10 cells were isolated, as previously described, using anti–Met-72 monoclonal antibodies and flow cytometry–coupled cell sorting (EPICS ELITE; Coulter Electronics, Hieleah, FL) [29]. Anti–Met-72 monoclonal antibodies, which react with a 72-kDa cell surface protein (Met-72) expressed at high density on B16M clones of high metastatic activity, were produced as described by Kimura and Xiang [30].

Invasive cells suspended in Krebs-Henseleit bicarbonate medium (pH 7.4) were centrifuged through a layer of silicone oil (AR200; Serva, Heidelberg, Germany). The presence of ^3H_2O (2.5 mCi/ml) (Amersham, Bucks, UK) in the cell suspension allows calculation, after centrifugation, of the radioactivity accumulated in the intracellular compartment [22].

Expression of Results and Statistical Significance

Data are presented as mean ± SD for the indicated number of different experiments. Statistical analyses were performed using Student's *t* test and $P < .05$ was considered significant.

Results

Plasma Levels of PTER and QUER

Depending on dietary habits, the human intake of flavones and flavonols (the most common flavonoids) is ~3 to 70 mg/day, mainly QUER (60–75%) (major sources include tea, wine, berries, apples, and onions) [31]. However, there are no reported estimations regarding PTER intake, which is present, for example, in extracts of the heartwood of *Pterocar marsupium*, which is used in Ayurvedic medicine for the treatment of diabetes, and in dark-skinned grapes (although quantitative studies have shown that for every 10 parts of RESV, there are only one to two parts of PTER) (Ref. [16] and references therein). As shown in Figure 1, after intravenous administration to mice of 20 mg/kg t-PTER or QUER (a dose that is representative for an adult human being of 70 kg body weight ~1000 times the maximum amount of PTER found in 1 kg of dark grapes, and ~20 times the maximum daily intake of QUER), their highest concentration in plasma (~95 μM PTER and ~46 μM QUER 5 minutes after administration) decreased to ~1 μM in 480 minutes (PTER) to 120 minutes (QUER). Following an identical protocol, we found previously that the highest RESV concentration in plasma (~43 μM 5 minutes after intravenous administration to rabbits) decreased rapidly to ~1 μM in 60 minutes [14]. We calculated a half-life of RESV in mouse plasma of ~10.2 minutes (Estrela et al., unpublished data). From the data in Figure 1, we calculated a half-life of PTER and QUER of ~77.9 and 20.1 minutes, respectively (Figure 1). Data reported in Figure 1 for each polyphenol

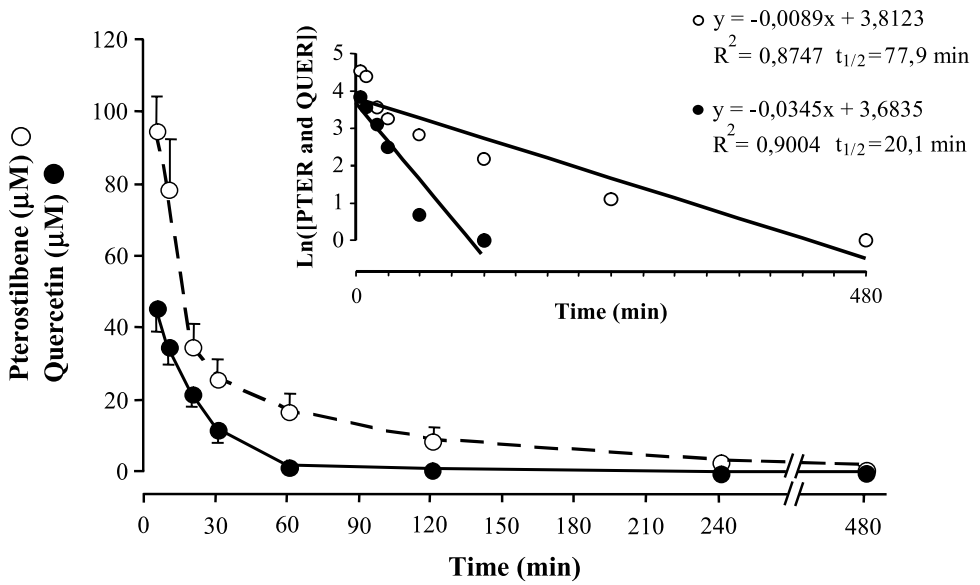

Figure 1. *Plasma levels and half-life of pterostilbene and quercetin after their intravenous administration to mice. Animals were treated with 20 mg of t-PTER or QUER per kilogram body weight. Plasma levels were determined as explained under Materials and Methods section. Results are mean ± SD for five to six mice per time point.*

were not significantly different when PTER and QUER were administered together (not shown). Total blood levels of PTER or QUER in mice were not significantly different from those reported above for plasma (not shown). At least 99% of the PTER measured in plasma or blood was in the *trans* form.

For comparison, t-PTER or QUER (20 mg/kg) was also administered orally. A mixture of ^{3}H-t-PTER (5 μCi/mouse) and unlabeled t-PTER or ^{14}C-QUER (2 μCi/mouse) and unlabeled QUER was administered in order to differentiate between free nonmodified polyphenols and their metabolites/conjugates generated under *in vivo* conditions. For calculations, free forms were measured by LC/MS-MS (under Materials and Methods section). Then, after correcting for dilutions, radioactivity in samples containing only free PTER or QUER was subtracted from the total radioactivity measured in an equivalent plasma sample. As shown in Table 1, after oral administration, plasma levels of PTER and QUER peaked at 60 and 10 minutes, respectively. However, total levels of PTER and QUER (free unchanged polyphenols plus their metabolites and conjugated forms) were very different. Total PTER concentration was > 10 μM between 30 and 240 minutes after administration, whereas total QUER levels only remained > 1 μM within the first 10 minutes (Table 1). During those time periods, free PTER represented a small percent of the total (15–35%), whereas free QUER (excepting the first 5 minutes) was almost undetectable (< 0.5%) (Table 1).

Extravascular Levels of PTER and QUER

In order to complement plasma/blood pharmacokinetics following intravenous administration (Figure 1), we also evaluated extravascular tissue bioavailability of PTER and QUER. As shown in Table 2, after their intravenous administration to mice, the highest content of PTER or QUER in the brain, lung, liver, and kidney was found within the first 5 minutes after administration (Table 2). Therefore, it appears that both polyphenols do not accumulate extravascularly and that their presence in different tissues (Table 2) parallels in time their bioavailability in the bloodstream (Figure 1). Nevertheless, it is important to remark the different pharmacokinetics obtained for both polyphenols when oral and intravenous administrations are compared (Figure 1 and Table 1). PTER and QUER were practically undetectable in plasma at 60 and 240 minutes, respectively, after their intravenous administration; whereas both polyphenols were detectable even 720 minutes after their oral administration. These facts are the obvious consequence of absorption and metabolism at the digestive tract, in which PTER and QUER must also be different (as suggested by the data in Table 1).

Inhibition of B16 Melanoma Cell Growth In Vitro

The highly aggressive B16 melanoma F10 (B16M-F10) is a model widely used to study metastatic spread and tissue invasion [21], and thus was selected for our studies. In the first set of experiments, the effect of t-PTER and QUER on B16M-F10 cell growth was followed *in vitro*. To mimic *in vivo* conditions after intravenous administration, we incubated B16M-F10 cells in the presence of t-PTER (40 μM) and/or QUER (20 μM) for a limited period (60 minutes) (this represents an approximate mean value of the concentrations of PTER and QUER measured in plasma during the first hour after intravenous administration of 20 mg/kg of each polyphenol) (Figure 2). For comparison, we also used t-RESV (12 μM; a similar criterion was followed to select this concentration; see data reported in Ref. [14]). Polyphenols were added to the incubation medium each 24 hours and, as indicated, were present only for 60 minutes. As shown in

Table 1. Plasma Levels of Pterostilbene and Quercetin after Their Oral Administration to Mice.

Time (min)	PTER		QUER	
	(μM)	(% Free)	(μM)	(% Free)
5	2.9 ± 0.6	67 ± 13	1.6 ± 0.3	22 ± 6
10	6.6 ± 1.8*	50 ± 10	2.3 ± 0.7	< 0.5*
30	11.1 ± 3.0*	35 ± 5*	0.6 ± 0.2*	< 0.5*
60	18.2 ± 2.7*	17 ± 6*	0.2 ± 0.1*	< 0.5*
120	13.3 ± 3.4*	15 ± 3*	0.07 ± 0.01*	< 0.5*
240	10.6 ± 1.2*	16 ± 4*	0.05 ± 0.02*	< 0.5*
480	7.1 ± 0.8*	14 ± 4*	0.05 ± 0.02*	< 0.5*
720	1.6 ± 0.5*	12 ± 2*	0.04 ± 0.01*	< 0.5*
1440	n.d.	n.d.	n.d.	n.d.

Animals were treated with 20 mg of t-PTER or QUER per kilogram body weight. A group of six to seven mice was sacrificed for each time point.
Nondetectable = n.d.
*$P < .01$ comparing data obtained at 10 to 1440 minutes *versus* those found 5 minutes after polyphenol administration.

Figure 2, t-PTER and QUER inhibited B16M-F10 growth by ~40 and 19%, respectively. However, when both were present, cancer growth inhibition increased to ~56%, which suggests a possible additive/synergic effect. To test this possibility, we performed dose–response studies (data not shown) and calculated the interaction index of the combination of t-PTER and QUER (see the Materials and Methods section) and found a value of 0.74 ± 0.05 (n = 5), which indicates synergy. In the experiments reported in Figure 2, cell cycle distribution (approximate percent of cells in G0/G1, S, and G2/M phases, n = 6, in all cases) was 58.0 ± 5.5, 22.4 ± 3.7, and 19.6 ± 2.6 in controls growing exponentially; 74.0 ± 4.4, 11.4 ± 1.7, and 14.6 ± 2.7 in t-PTER–treated cells; 65.3 ± 5.2, 15.8 ± 2.8, and 18.9 ± 2.0 in QUER-treated cells; and 77.7 ± 7.1, 13.2 ± 1.4, and 9.1 ± 1.6 in t-PTER– and QUER-treated cells (cell viability remained >95% in all cases). Therefore, despite their different percentages of tumor cell growth inhibition, both polyphenols tend to induce accumulation in G0/G1. In our experimental conditions, t-RESV did not affect significantly the rate of tumor cell growth (Figure 2). Moreover, t-RESV did not affect significantly the percentage of B16M-F10 growth inhibition (Figure 2) or the cell cycle distribution found in the presence of t-PTER and/or QUER.

Table 2. Extravascular Levels of Pterostilbene and Quercetin after Their Intravenous Administration to Mice.

Time (min)	Brain		Lung		Liver		Kidney	
	PTER	QUER	PTER	QUER	PTER	QUER	PTER	QUER
5	5 ± 1	4 ± 1	36 ± 6	15 ± 3	14 ± 4	9 ± 3	3 ± 1	1 ± 0.2
10	2 ± 0.5*	2 ± 0.4*	15 ± 3*	8 ± 2*	7 ± 1*	3 ± 1*	3 ± 0.3	1 ± 0.5
30	n.d.	n.d.	6 ± 1*	2 ± 0.6*	3 ± 0.5*	1 ± 0.2*	2 ± 0.4	n.d.
60	n.d.	n.d.	2 ± 1*	n.d.	n.d.	n.d.	1 ± 0.3*	n.d.

Animals were treated with 20 mg of t-PTER or QUER (containing 5 μCi of ^{3}H-t-PTER or 2 μCi of ^{14}C-QUER) per kilogram body weight. A group of four to five mice was sacrificed for each time point.
Nondetectable = n.d.
*$P < .01$ comparing data obtained at 10 to 60 minutes *versus* those found 5 minutes after polyphenol administration.

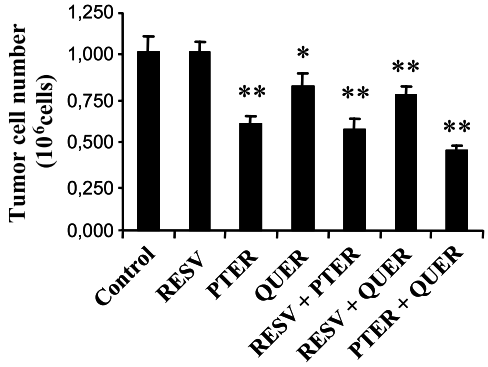

Figure 2. *In vitro inhibition of B16M-F10 cell growth by short-time exposure to resveratrol, pterostilbene, and/or quercetin. B16M-F10 cells were cultured for 72 hours. t-RESV (12 μM), t-PTER (40 μM), and QUER (20 μM) were added at 6, 30, and 54 hours of culture time, and were present each time for only 60 minutes. After the 60-minute period in the presence of polyphenols, the culture flasks were washed out (three times with PBS) and the medium was renewed. All points are mean ± SD for five to six independent experiments. *P < .05, **P < .01 compared to control values.*

Also for comparison, we incubated B16M-F10 cells in the presence of t-PTER and QUER at concentrations that represent an approximate mean value of the total level of each polyphenol measured in plasma within the first hour after oral administration (11 μM PTER and 1 μM QUER) (Table 1). Both polyphenols, as free forms, were present constantly in the incubation medium. Although both PTER and QUER follow metabolic transformations after oral administration, the use of free forms is a valid approach because their metabolites/conjugates are not expected to show stronger antitumor activity (e.g., Refs. [32,33]). However, under these conditions, t-PTER (11 μM) and/or QUER (1 μM) did not affect significantly the control rates of B16M-F10 cell growth *in vitro* (similar control rates reported in Figure 2) (data not shown). Total levels of free polyphenols added to the incubation medium did not change along the culture time, indicating that cancer cells do not metabolize/conjugate t-PTER or QUER (not shown).

Interaction between B16 Melanoma and Endothelial Cells In Vitro

In addition to the effect of PTER and QUER on tumor cell growth *in vitro*, other potential antimetastatic mechanisms were investigated. First, the interaction of B16M-F10 cells and the HSE was studied *in vitro*. Based on the results obtained above, we selected the short-term (60 minutes) exposure of metastatic cells to polyphenols [at the concentrations measured in plasma after their intravenous administration: t-RESV (12 μM), t-PTER (40 μM), and/or QUER (20 μM)]. Because the interaction of metastatic cells with endothelial and Kupffer cells activates local release of proinflammatory cytokines, which promote cancer cell adhesion to the endothelium and invasion [14,34], we investigated the effect of polyphenols on B16M-F10 cell adhesion to the HSE in the presence of TNF-α and IFN-γ (this cytokine combination fully activates the HSE; e.g., Ref. [20] and references therein) (Table 3). As previously reported [14], t-RESV inhibits tumor cell adhesion to the endothelium (~47%)

Table 3. Effect of Short-Time Exposure to Resveratrol, Pterostilbene, and/or Quercetin on the *In Vitro* Interaction between B16M-F10 Cells and the Vascular Endothelium.

Additions	Tumor Cell		Number of Penetrated Colonies Per cm^2
	Adhesion (%)	Cytotoxicity (% Adhered Cells)	
None	100 ± 15	15 ± 2	157 ± 17
RESV	53 ± 7*	12 ± 3	104 ± 12*
PTER	40 ± 6*	19 ± 3†	89 ± 9*
QUER	98 ± 11	52 ± 6*	106 ± 15*
RESV + PTER	32 ± 4*	17 ± 4	77 ± 8*
RESV + QUER	55 ± 7*	55 ± 7*	70 ± 7*
PTER + QUER	37 ± 5*	54 ± 5*	41 ± 5*

Twenty-four-hour cultured HSE cells [± polyphenol(s), added 12 hours after plating and removed by washing 60 minutes later] were cocultured with 72-hour cultured B16M cells [± polyphenol(s), as in Fig. 2]. Cytokines [100 U/ml TNF-α and 50 U/ml IFN-γ; see Ref. [20]] or vehicle (physiological saline) were added to the culture media 12 hours before starting cocultures. The ratio of tumor cells adhering to the HSE was ~1:1 in cytokine-treated cultures in the absence of polyphenols (a 100% adhesion rate was given to this value). In B16M endothelial cell adhesion experiments, 20 minutes after B16M addition to the HSE, the plates were washed as described under Materials and Methods section. In endothelium-induced B16M cytotoxicity assays, tumor cytotoxicity (expressed as the percentage of tumor cells that lost viability within the 4- to 6-hr period of incubation; see Materials and Methods section) was determined after 6 hours of incubation. During the 6-hour period of incubation, the percentage of HSE cell viability was 99–100% in all cases. All assays were performed in the absence or in the presence of t-RESV (12 μM), t-PTER (40 μM), and/or QUER (20 μM). Values represent mean ± SD of five to six different experiments in each case.
*$P < .01$ by comparing incubations in the presence and in the absence of polyphenol(s).
†$P < .05$.

without increasing HSE-induced metastatic cell cytotoxicity. A similar effect (~60% inhibition of adhesion) is found in the presence of t-PTER (Table 3). On the contrary, QUER increases HSE-induced B16M-F10 cell death (~48%) but without affecting the rate of adhesion (Table 3). As shown in Table 3, by combining t-PTER and QUER, we obtained the lowest percentage of B16M.F10 cell adhesion to the HSE and the highest percentage of cytotoxicity in the adhered cancer cells. Assaying the *in vitro* invasion of hepatic endothelial cell monolayers by B16M-F10 cells, we found a marked decrease (~74%) in the number of penetrated colonies in the presence of t-PTER and QUER (Table 3).

Adhesion of B16M-F10 cells to the HSE induces endothelial NO and H_2O_2 release, leading to metastatic cell killing [20]. We found that H_2O_2 was not cytotoxic in the absence of NO; however, NO-induced tumor cytotoxicity was increased by H_2O_2 due to the formation of potent oxidants such as $^{\bullet}OH$ and $^{-}ONOO$ radicals through a trace metal–dependent process [20]. We found that, during B16M-F10 and HSE interaction in the presence of t-PTER and QUER (both present *x*60 minutes as in Table 3), NO_x accumulated in the cultured medium during a 3-hour period was not significantly different from controls (7.5 ± 1.3 nmol/10^6 cells; $n = 6$). However, t-PTER and QUER decreased H_2O_2 generation from 70 ± 12 nmol/10^6 cells (controls) to 34 ± 10 nmol/10^6 cells ($n = 5–6$ in both cases, $P < .01$). Therefore, an increase in endothelial NO and H_2O_2 release cannot be argued as a potential antimetastatic mechanism in our model. Although, obviously, other mechanism(s) activated by t-PTER and/or QUER must favor the decrease in metastatic activity shown in Table 3.

Expression of Intercellular Adhesion Molecules

In order to further elucidate the underlying molecular mechanisms, we also used flow cytometry analysis to measure VLA-4 and VCAM-1 expression in B16M-F10 and HSE cells, respectively, cultured in the presence of t-PTER (40 μM) and/or QUER (20 μM). Interaction between VLA-4 on B16M cells and VCAM-1 on activated endothelial cells is a necessary step in the metastatic process [26]. As shown in Table 4, flow cytometric analysis revealed that B16M-F10 and HSE cells expressed high levels of VLA-4 and VCAM-1, respectively, on their surfaces, and that, as previously reported for t-RESV [14], t-PTER decreased VCAM-1 in HSE cells (Figure 3). We found no statistical differences when VCAM-1 levels determined after exposure to PTER or the combination of PTER and QUER were compared (not shown). This mechanism may explain the inhibitory effect of PTER on B16M-F10 and HSE intercellular adhesion.

Expression of Prodeath and Antideath Bcl-2 Genes in B16 Melanoma Cells

Recently, RT-PCR expression analysis of a *Bcl-2* family of genes revealed that B16M-F10 cells (high metastatic potential), compared with B16M-F1 cells (low metastatic potential), overexpressed preferentially Bcl-2 [35]. Therefore, because Bcl-2 overexpression can increase metastatic cell resistance against oxidative and nitrosative stress [35], changes in the expression of prodeath and/or antideath *Bcl-2* genes could be related to the increase in endothelium-induced B16M-F10 cytotoxicity elicited by QUER (Table 3). We studied this question by analyzing the effect of t-PTER and/or QUER on the expression of death-related *Bcl-2* genes. As shown in Table 5, t-PTER increases the expression of prodeath BAX (~2.2-fold) and decreases expression of antideath Bcl-2 (~2.2-fold). Besides, QUER increases the

Table 4. Effect of Pterostilbene and/or Quercetin on the Expression of VLA-4 on B16M-F10 Cells and of VCAM-1 on HSE Cells.

	ΔFL1			
	No Additions	PTER	QUER	PTER + QUER
B16M-F10	12 ± 3	16 ± 3	10 ± 2	14 ± 3
B16M-F10 + anti–VLA-4	159 ± 27	168 ± 31	144 ± 32	150 ± 21
HSE	36 ± 6	25 ± 6	30 ± 5	28 ± 4
HSE + anti–VCAM-1	266 ± 44	107 ± 19*	242 ± 53	116 ± 17*

VLA-4 and VCAM-1 expression was analyzed by flow cytometry as explained under Materials and Methods section. B16M-F10 and HSE cells [± polyphenol(s)] were cultured and then cocultured in the presence of TNF-α and IFN-γ, as indicated in the legend to Table 3. Cells were harvested (see under Materials and Methods section), washed twice in ice-cold fresh PBS, and resuspended in DMEM before starting incubations with antibodies. Assays were performed in the absence or in the presence of t-PTER (40 μM) and/or QUER (20 μM). Results are expressed as fluorescence intensity (ΔFL1) and represent mean ± SD of four to five different experiments in each case.
*$P < .01$ by comparing incubations in the presence and in the absence of polyphenol(s).

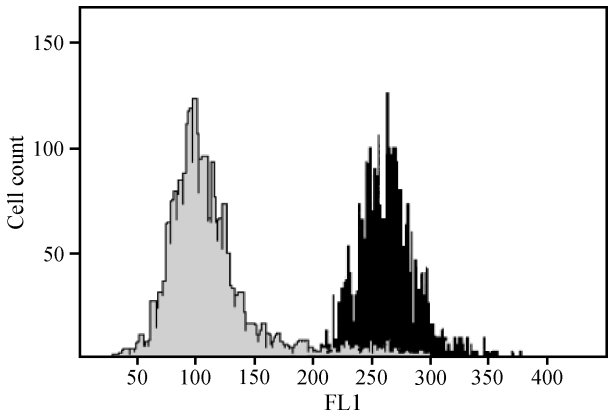

Figure 3. *Flow cytometric analysis of VCAM-1 on HSE cells. Flow cytometry was performed (see the legend to Table 4) on cultured endothelial cells incubated in the absence or in the presence of t-PTER (40 μM). Black histogram: control cells. Grey histogram: t-PTER–treated cells. Results shown are representative of five different experiments.*

expression of all prodeath genes analyzed (*BAX*, *BAK*, *BAD*, and *BID*) (e.g., *BAX*; ~2.5-fold) and decreases the expression of all antideath genes analyzed (*Bcl-2*, *Bcl-w*, and *Bcl-xL*) (e.g. *Bcl-2*; ~7.3 fold) (Table 5). Gene expression analysis was similar when data obtained in the presence of QUER or in the presence of t-PTER and QUER were compared (Table 5). These effects may explain the increase in tumor cytotoxicity elicited by the endothelium in the presence of t-PTER and QUER (Table 3).

Metastatic Growth in the Liver

Finally, the effect of PTER and/or QUER was also studied *in vivo*. For this purpose, mice were inoculated with control B16M-F10 or Bcl-2–overexpressing B16M-F10/Tet-Bcl-2 cells. Both cell subsets were previously cultured in the absence or in the presence of t-PTER and/or QUER. As shown in Table 6 and Figure 4, t-PTER and/or QUER decreases intracellular Bcl-2 levels; although in agreement with the data in Table 5, this effect was more evident in the presence of QUER. Besides, also in agreement with our results in Tables 3 and 4, t-PTER or t-PTER + QUER decreased the number of arrested B16M-F10 and B16M-F10/Tet-Bcl-2 cells (no significant differences were found when results obtained in the presence of PTER or the polyphenol combination were compared). However, given the different Bcl-2 levels between both cell subsets, QUER and t-PTER + QUER only decreased the percentage of intact arrested cells in control B16M-F10 cells (Table 6). In consequence, although untreated mice inoculated with B16M-F10 or B16M-F10/Tet-Bcl-2 cells showed similar rates

Table 5. Effect of Pterostilbene and/or Quercetin on the Expression of Prodeath and Antideath *Bcl-2* Genes in B16M-F10 Cells.

Gene	Additions			
	None	PTER	QUER	PTER + QUER
BAX	1.0 ± 0.1	2.2 ± 0.3*	2.5 ± 0.3*	2.5 ± 0.5*
BAK	1.2 ± 0.2	1.0 ± 0.1	1.6 ± 0.2†	1.3 ± 0.2
BAD	0.9 ± 0.1	1.1 ± 0.1	2.3 ± 0.3*	2.2 ± 0.3*
BID	1.0 ± 0.1	1.2 ± 0.2	1.5 ± 0.1*	1.5 ± 0.1*
Bcl-2	1.1 ± 0.2	0.5 ± 0.1*	0.15 ± 0.05*	0.15 ± 0.05*
Bcl-w	1.2 ± 0.1	0.9 ± 0.1†	0.8 ± 0.2*	0.8 ± 0.2*
Bcl-xL	1.2 ± 0.2	0.8 ± 0.2	0.6 ± 0.1*	0.7 ± 0.2*

B16M-F10 cells were cultured × 72 hours in the absence or in the presence of t-PTER (40 μM) and/or QUER (20 μM), as indicated in the caption to Fig. 2. The data, expressing fold change (see under Materials and Methods section for calculations), show mean values ± SD for five to six different experiments.
*$P < .01$ comparing polyphenols *versus* no additions.
†$P < .05$.

Table 6. Metastatic Growth in the Liver of Mice Intrasplenically Injected with B16M-F10 Cells Treated with Pterostilbene and Quercetin and Containing Different Bcl-2 Levels.

	Additions	Melanoma	
		B16M-F10	B16M-F10/ tet-Bcl-2
Intracellular Bcl-2 levels before inoculation (U/mg protein)	NONE	35 ± 5	160 ± 25
	PTER	21 ± 4*	151 ± 18†
	QUER	9 ± 3*	125 ± 13‡,†
	PTER + QUER	7 ± 2*	118 ± 16*,†
Number of arrested cells (average number per lobule)	NONE	45 ± 7	42 ± 6
	PTER	20 ± 5*	21 ± 4*
	QUER	46 ± 9	40 ± 7
	PTER + QUER	18 ± 4*	17 ± 3*
Intact cells (% of arrested cells)	NONE	83 ± 14	85 ± 13
	PTER	85 ± 17	91 ± 20
	QUER	52 ± 8*	87 ± 13†
	PTER + QUER	48 ± 10*	90 ± 17†
Metastasis density (number of foci/100 mm^3)	NONE	27 ± 5	29 ± 5
	PTER	18 ± 4*	15 ± 3*
	QUER	15 ± 4*	26 ± 5†
	PTER + QUER	7 ± 2*	20 ± 4‡,†
Metastasis volume (% liver volume)	NONE	22 ± 4	25 ± 6
	PTER	14 ± 4*	15 ± 3*
	QUER	12 ± 3*	24 ± 5†
	PTER + QUER	6 ± 2*	19 ± 5†
Host survival (days)	NONE	13 ± 2	12 ± 1
	PTER	15 ± 2	12 ± 2
	QUER	15 ± 1	13 ± 2
	PTER + QUER	27 ± 3*	14 ± 2†

B16M-F10 cells were culturedn × 72 hours in the absence or in the presence of t-PTER (40 M) and/or QUER (20 M), as indicated in the caption to Fig. 2. Bcl-2 levels in control (none under additions) and Tet-Bcl-2–treated B16M-F10 cells were measured, in 72-hour cultured tumor cells, before inoculation. The number of arrested cells displayed on the table was calculated at 60 minutes postinjection (no significant differences were found when measurements were performed at 30, 120, 180, 240, or 360 minutes postinjection; not shown). The number of intact cells was calculated at 6 hours postinjection. In *in vivo* microscopy experiments, data are mean ± SD for four to five independent tests. Metastatic growth in the liver was evaluated as indicated under Materials and Methods section and, in this case, mice were treated daily (×10 days) with 20 mg of t-PTER and 20 mg of QUER per kilogram body weight administered intravenously (data are mean ± SD of 25 mice per group). A similar procedure and identical number of mice per group were used to evaluate host survival. The significant test refers, for all groups, to the comparison between PTER + QUER and no additions (‡$P < .05$ and *$P < .01$), and also to the comparison between B16M-F10/Tet-Bcl-2 *vs* control B16M-F10 cells (†$P < .01$).

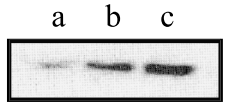

Figure 4. *Western blot analysis of Bcl-2 in B16M-F10 cells. B16M-F10 cells were cultured × 72 hours in the absence or in the presence of t-PTER (40 μM) or QUER (20 μM) (see the legend to Table 6). Lane a, QUER; lane b, t-PTER; lane c, control untreated cells.*

of metastatic growth in the liver and similar host survival, the effect of daily intravenous administration of t-PTER + QUER was more evident in control B16M-F10 cells: ~74% decrease in metastasis density and volume and a two-fold increase in host survival (Table 6). Although both PTER or QUER showed similar antimetastatic potential (~34% and a 45% decrease in metastasis density and volume, respectively), this was not associated with a significant increase in host survival. This fact suggests that PTER or QUER may be causing clonal selection of highly proliferating and resistant cancer cells [36,37], an aggressive cell subset whose growth may possibly be further decreased when both polyphenols are present. Obviously, an answer to this hypothesis will require further investigations.

Furthermore, it also possible that polyphenol combination that causes *in vitro* growth inhibition could also associate with a significant decrease in tumor cell volume within the liver metastases *in vivo*. To answer this question, we isolated B16M-F10 cells from their hepatic metastasis using anti–Met 72 monoclonal antibodies and flow cytometry–coupled cell sorting (see details of this recent methodology in Ortega et al. [29]). Then, cell volume of the isolated metastatic cells was quantified using ^3H_2O and centrifugation through a layer of silicone oil (see technical details in Ref. [22]). This procedure allowed calculation of the radioactivity accumulated within the intracellular compartment and yielded a volume of 3.7 ± 0.4 μl/mg dry weight (n = 5). This volume was not altered significantly in B16M-F10 cells isolated from PTER- and/or QUER-treated mice (not shown).

In conclusion, this is the first time that *in vivo* administration of natural polyphenols shows inhibition of metastatic growth of a highly malignant tumor and extension of host survival.

Discussion

Bioavailability and *in vivo* biologic efficacy are critical issues that must be correlated before drawing any conclusion on the potential health benefits of polyphenols [14,33,38]. As shown in Figure 2, where t-RESV, t-PTER, or QUER was tested, inhibition of B16M-F10 cell proliferation *in vitro* was stronger in the presence of t-PTER and QUER. Bioavailable concentrations of PTER and QUER, measured in plasma after oral administration, failed to inhibit B16M-F10 cell growth (even when concentrations of these polyphenols were constant along the culture time; see Inhibition of B16 Melanoma Cell Growth *In Vitro* section). However, bioavailable concentrations of PTER and QUER, measured in plasma after intravenous administration (Figure 1), inhibited tumor growth up to ~56% (even when both polyphenols were present only for 60 minutes for each 24 hours of culture) (Figure 2) without increasing the rate of cell death (cell viability remained > 95%, as in controls, in all cases). These experimental facts suggest that PTER and QUER may act as rapid molecular signals interfering, in a concentration-dependent fashion, in the mechanism of cell division. As described under Results section, most cultured B16M-F10 cells accumulated in G0/G1 in the presence of t-PTER and QUER. In fact, RESV (< 100 μM), the nonmethoxylated analog of PTER, also causes growth inhibition in a cell death–independent mechanism (see Ref. [39] for a review). For instance, in the presence of t-RESV, p53-, and p16-deficient CEM-C7H2, lymphocytic leukemia cells or human epidermoid carcinoma cells underwent G0/G1 phase arrest (as it occurs with the B16M-F10 melanoma model); whereas HL-60, human prostate cancer, human breast carcinoma, Caco-2, or rat and human hepatoma cell lines became arrested at S-phase [39]. Potential possible mechanisms for this growth-inhibitory activity are mentioned in the introduction. However, QUER arrests human leukemic T cells in G1 [40] and MCF-7 human breast cancer cells in G2/M; whereas in ovarian carcinoma cells, QUER attacks the cell cycle at the G1 and S phase boundary and inhibits 1-phosphatidylinositol 4-kinase activity [41]. Furthermore, it has been shown in human OCM-1 melanoma cells that the presence of a hydroxyl group at the 3′-position of the B-ring in QUER correlated to a G1 cell cycle arrest, whereas its absence in, for example, kaempferol or apigenin correlated to a G2 block [42]. This suggests, as it was proven in the case of RESV [15], that specific structural determinants are responsible for the antioxidant activity and the cell cycle effects of QUER. Moreover, as suggested above, there is an emerging view that flavonoids and their *in vivo* metabolites, and likely other polyphenols, may also exert modulatory effects in cells acting on, for example, phosphoinositide 3-kinase, Akt/protein kinase B, tyrosine kinases, protein kinase C, or mitogen-activated protein kinase signalling cascades [43]. Naturally, analysis of the signalling activity of PTER and QUER, although far beyond the aim of the present report, is a very interesting issue that deserves further studies.

In a previous report, we showed that *in vivo* administration of t-RESV (e.g., 20 mg/kg body weight given orally twice per day) was capable of decreasing B16M-F10 metastatic growth in the liver but without extending host survival [14]. RESV inhibited VCAM-1 expression in endothelial cells and, thereby, decreased the rate of the adhesion between metastatic and the vascular endothelium [14]. However, RESV did not affect endothelium-induced tumor cytotoxicity [14], and may possibly cause clonal selection of highly proliferating and resistant cancer cells (Refs. [20,44] and references therein). Based on these facts, on the differences in bioavailability, and on the data shown in Figure 2, we selected the combination of PTER and QUER to study its effect on metastatic progression. As shown in Table 3, the effect of t-PTER, QUER, t-RESV, or their combinations on the *in vitro* interaction between B16M-F10 cells and the vascular endothelium was investigated. Parallel to the effect on B16M-F10 cells growing *in vitro* (Figure 2), the association between PTER and QUER was the best in decreasing the percentage of B16M-F10 cells adhered to the HSE and in increasing the percentage of endothelium-induced tumor cytotoxicity (Table 3). In consequence, t-PTER and QUER decreased by ~74% the formation of tumor colonies in an *in vitro* test of invasion (Table 3). The antimetastatic mechanisms include inhibition of VCAM-1 expression in the HSE by PTER (possibly mediated by NO if PTER works as RESV-inducing nitric oxide synthase) [45],

which consequently decreases B16M-F10 cell adhesion to the endothelium through VLA-4 (Table 4); and QUER- and PTER-induced changes in expression of Bcl-2–related proteins (upregulation of proapoptotic and downregulation of antiapoptotic proteins) in B16M-F10 cells (Table 5), which sensitizes them to HSE-induced cytotoxicity (Table 6).

Selectins, integrins, cadherins, and immunoglobulins, as well as unclassified molecules, have been demonstrated to govern the adhesive interactions between metastatic cells and the vascular endothelium. Initial contact between metastatic cells and the endothelium ("docking") is weak and transient, and likely mediated by carbohydrate–carbohydrate recognition [34]. The mechanism of B16M-HSE interaction includes mannose receptor–mediated melanoma cell attachment to the HSE, which subsequently causes cytokine (TNFα, IL-1B, and IL-18) and NO/H_2O_2 release, VCAM-1–dependent adherence (reinforcing or "locking" the initial intercellular binding), and melanoma growth factors release by the HSE [46]. Involvement of the VLA-4 integrin on melanoma locking adhesion to endothelial through VCAM-1 is a well-described mechanism. For instance, Garofalo et al. [47] showed that A375M human melanoma cells expressed high levels of VLA-4 and preferentially adhered to a surface coated with vascular cell adhesion molecule 1 (VCAM-1), the ligand for VLA-4 on activated endothelial cells. Thus, we focussed on VLA-4 and VCAM-1 as a critical step in the mechanisms preceding B16M invasion. Nevertheless, this is not excluding *per se* other molecular mechanisms applying to this model, or other intercellular adhesion molecules binding other types of metastatic cells to the vascular endothelium [34]. To answer which is the relative importance of VCAM-1/VLA-4 interaction between HSE and B16M-F10 cells, we used two parallel approaches. We administered antimouse VCAM-1 monoclonal antibodies (50 μg) intraportally to mice 60 minutes before B16M-F10 inoculation. This caused an 89% decrease in the number of arrested cancer cells in the liver sinusoids (from 45 ± 7 to 5 ± 2; $n = 4$, $P < .01$; Table 6). Besides, when B16M-F10 cells were preincubated for 1 hour in the presence of antimouse VLA-4 monoclonal antibodies (10^6 cells/μg antibody) before inoculation, the number of arrested cancer cells in the microvasculature also decreased by an 85% (from 45 ± 7 to 7 ± 3, $n = 4$, $P < .01$; Table 6).

Bcl-2 overexpression prevents the QUER- and PTER-dependent increase in metastatic B16M-F10 cell death caused by the HSE *in vivo* (Table 6). Thus, Bcl-2 itself appears as a critical regulator of B16M-F10 resistance against HSE-induced damage. *In vitro* experiments have shown that QUER is an apoptosis inducer in, for example, human promyeloleukemic HL-60 cells [48] or BL6 murine melanoma cells [49], although only in BL6 cells was a QUER-dependent downregulation of Bcl-2 expression suggested as a causal agent. Furthermore, given the structural relationship between PTER and RESV, these results also appear in agreement with others reporting inhibition of RESV-induced apoptosis by Bcl-2, and downregulation of Bcl-2 and upregulation of BAX upon exposure to RESV [50]. Although recent data suggest that RESV-mediated apoptosis is independent of BAX (as suggested above; Table 6), as gene knockout of BAX did not alter tumor cell sensitivity to RESV [3,51]. In addition, other potential antimetastatic effects of PTER and QUER need to be explored (e.g., interestingly, RESV and QUER have been shown to inhibit angiogenesis *in vitro* in a concentration-dependent manner) (6–100 μM) [52].

Can possible clinical applications be derived from our study? To show that natural polyphenols, such as t-PTER and QUER, inhibit *in vivo* metastatic growth of a highly malignant tumor leading to longer host survival, we used daily intravenous administration of high doses (20 mg/kg body weight administered once a day). However, at this point, different protocols must be naturally considered. For instance, if it is shown to be more effective and nontoxic for humans, the dosing could be scaled up. In addition, our results do not rule out possible benefits of using oral administration. In fact, t-RESV inhibits VCAM-1 expression at very low concentrations (1 μM) [14]. Nevertheless, as remarked by Goldberg et al. [33] and taking into account the *in vivo* metabolism of these small polyphenols (e.g., Refs. [53,54]), investigations of this nature should focus upon the benefits of their conjugates (e.g., glucuronides and sulfates). Moreover, doses required to inhibit metastatic growth may depend on the cell type. Besides, association of t-PTER and QUER could also be useful in other oxidative stress-related pathologies (e.g., diabetes, arteriosclerosis, neurodegenerative diseases, or ischemic heart) [55] where doses required to obtain benefits could be similar or entirely different.

In conclusion, our findings open a new window for possible applications of polyphenol associations in cancer therapy. Moreover, because polyphenol administration can be combined with biotherapy, cytotoxic drugs, and/or ionizing radiation, the mechanisms described in this report may have useful applications to improve therapy against metastatic melanoma and, possibly, against other malignant tumor types.

References

[1] Yang CS, Landau JM, Huang MT, and Newmark HL (2001). Inhibition of carcinogenesis by dietary polyphenolic compounds. *Annu Rev Nutr* **21,** 381–406.

[2] Ross JA and Kasum CM (2002). Dietary flavonoids: bioavailability, metabolic effects, and safety. *Annu Rev Nutr* **22,** 19–34.

[3] Pervaiz S (2003). Resveratrol: from grapevines to mammalian biology. *FASEB J* **17,** 1975–1985.

[4] Jang M, Cai L, Udeani GO, Slowing KV, Thomas CF, Beecher CW, Fong HH, Farnsworth NR, Kinghorn AD, Mehta RG, et al. (1997). Cancer chemopreventive activity of resveratrol, a natural product derived from grapes. *Science* **275,** 218–220.

[5] Fontecave M, Lepoivre M, Elleingand E, Gerez C, and Guittet O (1998). Resveratrol, a remarkable inhibitor of ribonucleotide reductase. *FEBS Lett* **421,** 277–279.

[6] Sun NJ, Woo SH, Cassady JM, and Snapka RM (2003). DNA polymerase and topoisomerase II inhibitors from *Psoralea corylifolia*. *J Nat Prod* **66,** 734.

[7] Stewart JR, Ward NE, Ioannides CG, and O'Brian CA (1999). Resveratrol preferentially inhibits protein kinase C–catalyzed phosphorylation of a cofactor-independent, arginine-rich protein substrate by a novel mechanism. *Biochemistry* **38,** 13244–13251.

[8] Subbaramaiah K, Chung WJ, Michaluart P, Telang N, Tanabe T, Inoue H, Jang M, Pezzuto JM, and Dannenberg AJ (1998). Resveratrol inhibits cyclooxygenase-2 transcription and activity in phorbol ester–treated human mammary epithelial cells. *J Biol Chem* **273,** 21875–21882.

[9] Sauer H, Wartenberg M, and Hescheler J (2001). Reactive oxygen species as intracellular messengers during cell growth and differentiation. *Cell Physiol Biochem* **11,** 173–186.

[10] Clement MV, Hirpara JL, Chawdhury SH, and Pervaiz S (1998). Chemopreventive agent resveratrol, a natural product derived from grapes, triggers CD95 signaling–dependent apoptosis in human tumor cells. *Blood* **92,** 996–1002.

[11] She QB, Bode AM, Ma WY, Chen NY, and Dong Z (2001). Resveratrol-induced activation of p53 and apoptosis is mediated by extracellular-signal–regulated protein kinases and p38 kinase. *Cancer Res* **61,** 1604–1610.

[12] Tinhofer I, Bernhard D, Senfter M, Anether G, Loeffler M, Kroemer G, Kofler R, Csordas A, and Greil R (2001). Resveratrol, a tumor-suppressive compound from grapes, induces apoptosis *via* a novel mitochondrial pathway controlled by Bcl-2. *FASEB J* **15,** 1613–1615.

[13] Scarlatti F, Sala G, Somenzi G, Signorelli P, Sacchi N, and Ghidoni R (2003). Resveratrol induces growth inhibition and apoptosis in metastatic breast cancer cells *via de novo* ceramide signaling. *FASEB J* **17,** 2339--2341.

[14] Asensi M, Medina I, Ortega A, Carretero J, Bano MC, Obrador E, and Estrela JM (2002). Inhibition of cancer growth by resveratrol is related to its low bioavailability. *Free Radic Biol Med* **33,** 387–398.

[15] Stivala LA, Savio M, Carafoli F, Perucca P, Bianchi L, Maga G, Forti L, Pagnoni UM, Albini A, Prosperi E, et al. (2001). Specific structural determinants are responsible for the antioxidant activity and the cell cycle effects of resveratrol. *J Biol Chem* **276,** 22586–22594.

[16] Rimando AM, Cuendet M, Desmarchelier C, Mehta RG, Pezzuto JM, and Duke SO (2002). Cancer chemopreventive and antioxidant activities of pterostilbene, a naturally occurring analogue of resveratrol. *J Agric Food Chem* **50,** 3453–3457.

[17] Lamson DW and Brignall MS (2000). Antioxidants and cancer: Part 3. Quercetin. *Altern Med Rev* **5,** 196–208.

[18] Tuck KL, Tan HW, and Hayball PJ (2000). A simple procedure for the deuteriation of phenols. *J Label Compd Radiopharm* **43,** 817–823.

[19] Navarro J, Obrador E, Pellicer JA, Aseni M, Vina J, and Estrela JM (1997). Blood glutathione as an index of radiation-induced oxidative stress in mice and humans. *Free Radic Biol Med* **22,** 1203–1209.

[20] Carretero J, Obrador E, Esteve JM, Ortega A, Pellicer JA, Sempere FV, and Estrela JM (2001). Tumoricidal activity of endothelial cells. Inhibition of endothelial nitric oxide production abrogates tumor cytotoxicity induced by hepatic sinusoidal endothelium in response to B16 melanoma adhesion *in vitro. J Biol Chem* **276,** 25775–25782.

[21] Anasagasti MJ, Martin JJ, Mendoza L, Obrador E, Estrela JM, McCuskey RS, and Vidal-Vanaclocha F (1998). Glutathione protects metastatic melanoma cells against oxidative stress in the murine hepatic microvasculature. *Hepatology* **27,** 1249–1256.

[22] Carretero J, Obrador E, Anasagasti MJ, Martin JJ, Vidal-Vanaclocha F, and Estrela JM (1999). Growth-associated changes in glutathione content correlate with liver metastatic activity of B16 melanoma cells. *Clin Exp Metastasis* **17,** 567–574.

[23] Ohigashi H, Shinkai K, Mukai M, Ishikawa O, Imaoka S, Iwanaga T, and Akedo H (1989). *In vitro* invasion of endothelial cell monolayer by rat ascites hepatoma cells. *Jpn J Cancer Res* **80,** 818–821.

[24] Berenbaum MC (1985). The expected effect of a combination of agents: the general solution. *J Theor Biol* **114,** 413–431.

[25] Braman RS and Hendrix SA (1989). Nanogram nitrite and nitrate determination in environmental and biological materials by vanadium (III) reduction with chemiluminescence detection. *Anal Chem* **61,** 2715–2718.

[26] Okahara H, Yagita H, Miyake K, and Okumura K (1994). Involvement of very late activation antigen 4 (VLA-4) and vascular cell adhesion molecule (VCAM-1) in tumor necrosis factor alpha enhancement of experimental metastasis. *Cancer Res* **54,** 3233–3236.

[27] Obrador E, Carretero J, Esteve JM, Pellicer JA, Pascual A, Petschen I, and Estrela JM (2001). Glutamine potentiates TNF-alpha–induced tumor cytotoxicity. *Free Radic Biol Med* **31,** 642–650.

[28] Eissa S and Seada LS (1998). Quantitation of bcl-2 protein in bladder cancer tissue by enzyme immunoassay: comparison with Western blot and immunohistochemistry. *Clin Chem* **44,** 1423–1429.

[29] Ortega AL, Carretero J, Obrador E, Gambini J, Asensi M, Rodilla V, and Estrela JM (2003). Tumor cytotoxicity by endothelial cells. Impairment of the mitochondrial system for glutathione uptake in mouse B16 melanoma cells that survive after *in vitro* interaction with the hepatic sinusoidal endothelium. *J Biol Chem* **278,** 13888–13897.

[30] Kimura AK and Xiang JH (1986). High levels of Met-72 antigen expression: correlation with metastatic activity of B16 melanoma tumor cell variants. *J Natl Cancer Inst* **76,** 1247–1254.

[31] Rimm EB, Katan MB, Ascherio A, Stampfer MJ, and Willett WC (1996). Relation between intake of flavonoids and risk for coronary heart disease in male health professionals. *Ann Intern Med* **125,** 384–389.

[32] Day AJ, Bao Y, Morgan MR, and Williamson G (2000). Conjugation position of quercetin glucuronides and effect on biological activity. *Free Radic Biol Med* **29,** 1234–1243.

[33] Goldberg DM, Yan J, and Soleas GJ (2003). Absorption of three wine-related polyphenols in three different matrices by healthy subjects. *Clin Biochem* **36,** 79–87.

[34] Orr FW, Wang HH, Lafrenie RM, Scherbarth S, and Nance DM (2000). Interactions between cancer cells and the endothelium in metastasis. *J Pathol* **190,** 310–329.

[35] Ortega A, Ferrer P, Carretero J, Obrador E, Asensi M, Pellicer JA, and Estrela JM (2003). Down-regulation of glutathione and Bcl-2 synthesis in mouse B16 melanoma cells avoids their survival during interaction with the vascular endothelium. *J Biol Chem* **278,** 39591–39599.

[36] Carretero J, Obrador E, Esteve JM, Ortega A, Pellicer JA, Sempere FV, and Estrela JM (2001). Tumoricidal activity of endothelial cells. Inhibition of endothelial nitric oxide production abrogates tumor cytotoxicity induced by hepatic sinusoidal endothelium in response to B16 melanoma adhesion *in vitro. J Biol Chem* **276,** 25775–25782.

[37] Fidler IJ (1989). Origin and biology of cancer metastasis. *Cytometry* **10,** 673–680.

[38] Fremont L (2000). Biological effects of resveratrol. *Life Sci* **66,** 663–673.

[39] Soleas GJ, Diamandis EP, and Goldberg DM (2001). The world of resveratrol. *Adv Exp Med Biol* **492,** 159–182.

[40] Yoshida M, Yamamoto M, and Nikaido T (1992). Quercetin arrests human leukemic T-cells in late G1 phase of the cell cycle. *Cancer Res* **52,** 6676–6681.

[41] Shen F, Herenyiova M, and Weber G (1999). Synergistic down-regulation of signal transduction and cytotoxicity by tiazofurin and quercetin in human ovarian carcinoma cells. *Life Sci* **64,** 1869–1876.

[42] Casagrande F and Darbon JM (2001). Effects of structurally related flavonoids on cell cycle progression of human melanoma cells: regulation of cyclin-dependent kinases CDK2 and CDK1. *Biochem Pharmacol* **61,** 1205–1215.

[43] Williams RJ, Spencer JP, and Rice-Evans C (2004). Flavonoids: antioxidants or signalling molecules? *Free Radic Biol Med* **36,** 838–849.

[44] Fidler IJ (1989). Origin and biology of cancer metastasis. *Cytometry* **10,** 673–680.

[45] Hsieh TC, Juan G, Darzynkiewicz Z, and Wu JM (1999). Resveratrol increases nitric oxide synthase, induces accumulation of p53 and p21 (WAF1/CIP1), and suppresses cultured bovine pulmonary artery endothelial cell proliferation by perturbing progression through S and G2. *Cancer Res* **59,** 2596–2601.

[46] Mendoza L, Olaso E, Anasagasti MJ, Fuentes AM, and Vidal-Vanaclocha F (1998). Mannose receptor–mediated endothelial cell activation contributes to B16 melanoma cell adhesion and metastasis in liver. *J Cell Physiol* **174,** 322–330.

[47] Garofalo A, Chirivi RG, Foglieni C, Pigott R, Mortarini R, Martin-Padura I, Anichini A, Gearing AJ, Sanchez-Madrid F, Dejana E, et al. (1995). Involvement of the very late antigen 4 integrin on melanoma in interleukin 1–augmented experimental metastases. *Cancer Res* **55,** 414–419.

[48] Shen SC, Chen YC, Hsu FL, and Lee WR (2003). Differential apoptosis-inducing effect of quercetin and its glycosides in human promyeloleukemic HL-60 cells by alternative activation of the caspase 3 cascade. *J Cell Biochem* **89,** 1044–1055.

[49] Zhang X, Xu Q, and Saiki I (2000). Quercetin inhibits the invasion and mobility of murine melanoma B16-BL6 cells through inducing apoptosis *via* decreasing Bcl-2 expression. *Clin Exp Metastasis* **18,** 415–421.

[50] Tessitore L, Davit A, Sarotto I, and Caderni G (2000). Resveratrol depresses the growth of colorectal aberrant crypt foci by affecting bax and p21(CIP) expression. *Carcinogenesis* **21,** 1619–1622.

[51] Mahyar-Roemer M, Kohler H, and Roemer K (2002). Role of Bax in resveratrol-induced apoptosis of colorectal carcinoma cells. *BMC Cancer* **2,** 27.

[52] Igura K, Ohta T, Kuroda Y, and Kaji K (2001). Resveratrol and quercetin inhibit angiogenesis *in vitro. Cancer Lett* **171,** 11–16.

[53] Bravo L (1998). Polyphenols: chemistry, dietary sources, metabolism, and nutritional significance. *Nutr Rev* **56,** 317–333.

[54] Walle T (2004). Absorption and metabolism of flavonoids. *Free Radic Biol Med* **36,** 829–837.

[55] Davies KJ (1995). Oxidative stress: the paradox of aerobic life. *Biochem Soc Symp* **61,** 1–31.